Indonesian Physical Review

Volume 09 Issue 01, January 2026 P-ISSN: 2615-1278, E-ISSN: 2614-7904

Synthesis of Nanohydroxyapatite from Bukit Jimbaran Limestone

Gede Arya Amerta^{1*}, Ida Bagus Putu Mardana^{1*}, Putu Yasa^{1*}

¹ Department of Physics and Science Education, Faculty of Mathematics and Natural Sciences, Ganesha University of Education, Indonesia

Corresponding Authors E-mail: arya.amerta@undiksha.ac.id, putu.mardana@undiksha.ac.id, pt.yasa@undiksha.ac.id

Article Info

Article info:

Received: 02-08-2025 Revised: 25-10-2025 *Accepted:* 30-10-2025

Keywords:

HAp; precipitation; crystallinity; particle morphology; functional groups

How To Cite:

G. A. Amerta, I. B. P. Mardana, and P. Yasa "Synthesis of Nanohydroxyapatite from Bukit Jimbaran Limestone", Indonesian Physical Review, vol. 9, no. 1, p 27-38, 2026.

DOI:

https://doi.org/10.29303/ip r.v9i1.548.

Abstract

The global demand for biocompatible biomimetic materials drives the development of nanohydroxyapatite (HAp) for applications. This study aims to synthesize nanohydroxyapatite (Ca10(PO4)6(OH)2) from Bukit Jimbaran limestone, Bali, through a precipitation method. XRF analysis shows that the limestone contains 99.62% CaO, which is the main source of calcium. FTIR results detect the presence of phosphate (PO_4^{3-}) , carbonate (CO_3^{2-}) , calcium oxide (CaO), and hydroxyl (OH⁻) groups, confirming the formation of the typical HAp structure. The XRD diffraction pattern showed good agreement with JCPDS 09-0432, with major peaks on the (211), (112), and (300) planes, lattice parameters a = b = 9.45 Å and c = 6.85 Å, an average crystallite size of 8.70 nm, and a crystallinity of 92.88%. SEM-EDX analysis revealed agglomerated particle morphology, with a Ca content of 32.0 wt.% and a P content of 14.0 wt.%. The high crystallinity and very small crystallite size confirm the potential of this synthesized HAp to enhance bioactivity and accelerate bone integration, making Jimbaran limestone HP a strong candidate in the biomedical sector.



Copyright (c) 2026 by Author(s), This work is licensed under a Creative Commons Attribution-ShareAlike 4.0 International License.

Introduction

Nanohydroxyapatite (Ca10(PO4)6(OH)2) has received special attention in the fields of materials and medicine due to its superior bioactive, biocompatible, and osteoconductive properties that resemble the hard tissues of the human body [1,2,3]. The synthesis of HAp from limestone into a relevant topic for development, considering its very abundant availability, very low cost, and environmentally friendly characteristics [4,5]. Nanohydroxyapatite has superior biological properties because its chemical composition is very close to that of body tissues [6,7], and its functionality can be enhanced through doping processes with various elements [8,9,10]. In the medical field, HAp is widely used applied in the manufacture of bone and dental implants [11,12], where its biological properties allow for better control and high efficiency in clinical applications [13,14].

Various research was conducted in improve the effectiveness and efficiency of HAp materials. Research by [15] synthesized $Ca_{10}(PO_4)_6(OH)_2$ from ale-ale shells through a double stirring precipitation method with a crystallinity of 90.12% and identification of phosphate groups at wave numbers 1092.02; 1038.29; and 571.71 cm⁻¹, although the morphology showed agglomeration. Research by [16] used bovine bone (Bos taurus) as a precursor of HAp through calcination at 900 °C for 6 hours, which resulted in 95% crystallinity and OH^- , PO_4^{3-} , and CO_3^{2-} functional groups. Meanwhile, research by [17] utilized Pahae limestone, North Sumatra, as the basic material for HAp synthesis. FTIR results identified PO_4^{3-} (580.32 and 1131.96 cm⁻¹), $CaO(1657.106 \text{ cm}^{-1})$, CO_3^{2-} (1400.08 cm⁻¹), and OH^- (3412.48 cm⁻¹), while XRD characterization showed the highest intensity peak on the (211) plane, with lattice parameters a = b = 9.4232 Å and c = 6.8833 Å. SEM morphology at 2500x magnification showed the presence of HAp particle agglomeration.

The synthesis method and parameters plays a crucial role in getting the size, morphology, and crystallinity of HAp. These parameters directly affect the properties of Ca₁₀(PO₄)₆(OH)₂ synthesized from limestone. Commonly used methods include sol-gel, hydrothermal, emulsion, precipitation, and flux methods [18]. This research uses precipitation techniques because it is relatively simple, economical, and efficient in obtaining Ca₁₀(PO₄)₆(OH)₂ powder from natural materials [19], and is known to be able to produce nano-sized particles with relatively uniform morphological control [20].

Limestone is a natural source rich in calcium carbonate (CaCO₃), which after calcination at a temperature of 800°C will decompose into calcium oxide (CaO), the main precursor in synthesizing HAp. One of the areas with abundant limestone reserves is Bukit Jimbaran, Badung-Bali, which is dominated by CaCO₃ and CaO. Geologically, Bukit Jimbaran is a Tertiary-aged coastal tropical karst area, composed of reefs, marl, and fossils. Analysis shows that Bukit Jimbaran limestone has very high CaO purity (>95%) with small impurities such as Mg and Si, which act as natural doping in the HAp structure. The presence of this natural doping is important because it can increase bioactivity and thermal stability [21].

Although there has been much research on HAp synthesis from biominerals such as shells, cow bones, and Pahae limestone, to date there has been no research specifically utilizing Bukit Jimbaran limestone as a precursor. In fact, its unique geological properties produce a more regular calcite crystal structure, potentially producing HAp with higher crystallinity and a more uniform crystal size distribution than other sources. Thus, this research offers novelty through the use of Bukit Jimbaran limestone as a natural calcium source for HAp synthesis, while also providing a scientific contribution to the development of biomaterials based on local resources.

Experimental Method

This study used a precipitation method, with the main material being pure white limestone from Bukit Jimbaran, Bali, as a calcium precursor. The reagents used were: (1) ammonia/NH₄OH (Merck, Germany, p.a. grade \geq 25%); (2) phosphoric acid/H₃PO₄ (Merck, Germany, 85%); (3) aquabidest (Brataco, Indonesia) as a solvent; and (4) aquadest (Brataco, Indonesia) for washing samples and equipment. All materials were used directly without

further purification. The selection of chemicals with high purity was intended to maintain the reproducibility of the results.

The equipment used in the research included: (1) drying oven (Kirin, Indonesia); (2) calcination furnace (FB1410M-33, USA); (3) magnetic stirrer (IKA C-MAG HS7, Germany); (4) pH meter (Hanna Instruments HI2211, Romania); and (5) agate mortar (ISOLAB, Germany). In addition, the characterization tools used included: (1) XRF (PANalytical Minipal 4, Netherlands); (2) XRD (Bruker D6 PHASER, Germany); (3) FTIR (Shimadzu IR Prestige-21, Japan); and (4) SEM-EDX (Thermo Scientific Axia ChemiSEM, USA). The HAp synthesis process using precipitation technique is described in detail in five stages as follows.

Preparation of calcium precursor by grinding Bukit Jimbaran limestone into powder, then calcining at 850°C for 4 hours to remove organic compounds and produce CaO. The temperature of 850°C was chosen because it is in the optimum range of decomposition of CaCO₃ into CaO without causing excessive sintering that can reduce the reactivity of CaO. Next, the calcined powder was characterized using XRF to determine the content of CaO and impurities.

$$CaCO_3 \rightarrow CaO + CO_2 \uparrow$$
 (1)

The Ca(OH)₂ mixture was prepared by mixing 12.46 grams of calcined CaO into 100 mL of aquabidest, stirring at 250 rpm for 1 hour.

$$CaO + H_2O \to Ca(OH)_2 \tag{2}$$

Hydroxyapatite (Hap) synthesis was carried out by mixing Ca(OH)₂ solution (100 mL) into 100 mL of 1.333 M H₃PO₄ solution (the result of 85% H₃PO₄ dilution) while stirring at 250 rpm for 1 hour. The synthesis was continued at 60°C for 2 hours, with the pH of the mixture kept constant at pH 10 using NH₄OH. The choice of pH 10 was based on a report [38] that these moderately alkaline conditions support the hydroxyapatite phase at a Ca/P ratio approaching stoichiometry of 1.67.

$$10Ca(OH)_2 + 6H_3PO_4 \to Ca_{10}(PO_4)_6(OH)_2 + 18H_2O$$
(3)

The final stage includes settling the mixture for 24 hours, filtering, washing three times with distilled water, then dried in an oven at 110°C for 2 hours. The dried precipitate was then sintered at 900°C for 2 hours to increase crystallinity.

Characterization of Hap products was carried out using FTIR to identify functional groups $(PO_4^{3-}, CaO, CO_3^{2-}, OH^-)$; XRD to determine the crystal structure, lattice parameters, crystallite size, and crystallinity; and SEM-EDX to analyze particle morphology and elemental composition. In the XRD analysis, crystallite size is calculated using the Scherrer equation [31] and the percentage of crystallinity using the Landi method [32].

$$D = \frac{\kappa\lambda}{\beta\cos\theta} \tag{4}$$

$$X_c(\%) = 100 \times \left[1 - \frac{V_{112/300}}{I_{300}}\right] \tag{5}$$

The flow of implementation of nanohydroxyapatite synthesis research is briefly presented in Figure 1.

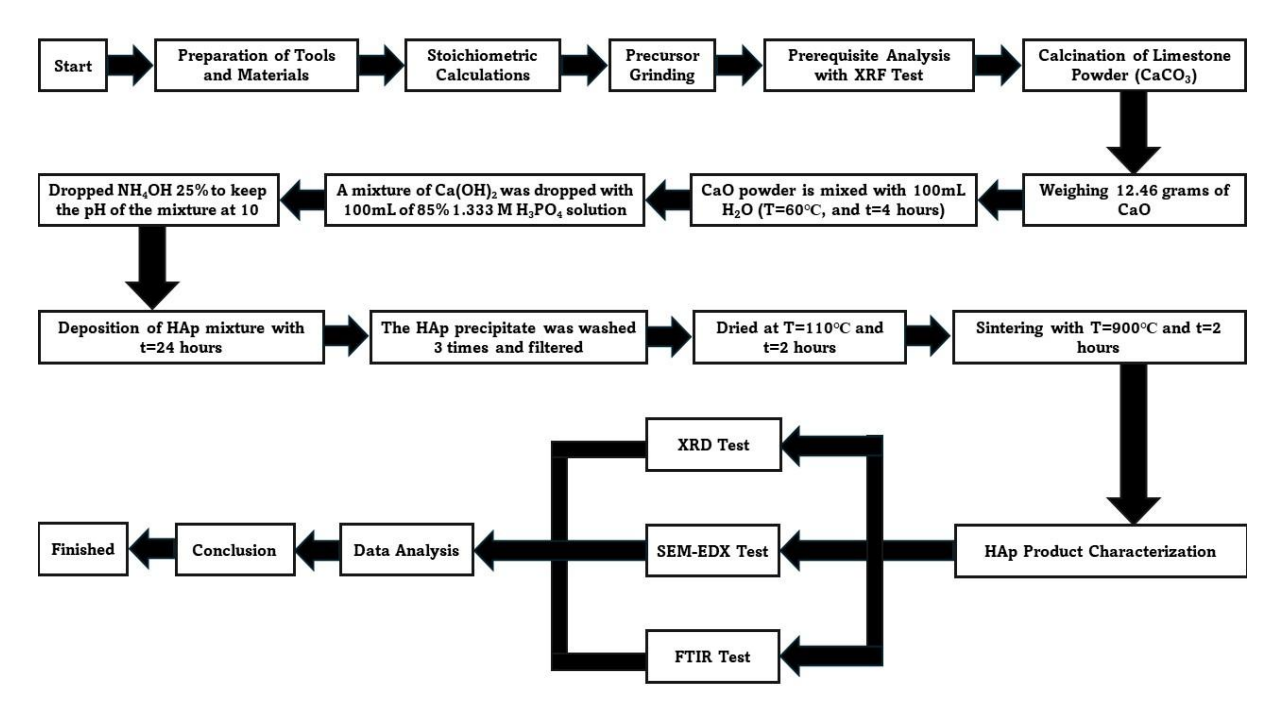


Figure 1. Flowchart of the Research Procedures

Result and Discussion

To ensure the success of the synthesis of nanohydroxyapatite from Bukit Jimbaran limestone, analysis was carried out using XRF, FTIR, XRD, and SEM-EDX. XRF analysis to determine the purity of the CaO content in limestone, the main precursor. The XRF test results for the Bukit Jimbaran limestone powder are shown in Table 1.

Element	CaO	Fe ₂ O ₃	CuO	Lu_2O_3
Percentage of Jimbaran Limestone Elements (%)	99.62	0.16	0.036	0.18
Percentage of Cikembar Limestone (%) [22]	55.84	0.45	-	-
Percentage of Leang-Leang Limestone (%) [23]	54.23	0.441	-	-

Table 1. XRF Test Results of Bukit Jimbaran Limestone Powder

The XRF results indicate a CaO content of 99.62%, with very low impurity content (Fe₂O₃, CuO, and Lu₂O₃). This purity is significantly higher than that of limestone from Cikembar (55.84%) [22] and the Leang-Leang area (54.23%) [23]. The high CaO content of the Bukit Jimbaran limestone is an important and beneficial factor because it facilitates the formation of the HAp phase and increases the product's crystallinity [24,25].

FTIR analysis to identify the typical functional groups of nanohydroxyapatite, through the identification of HAp compound groups, namely PO₄³⁻, CaO, CO₃²⁻, and OH⁻, as shown in Figure 2.

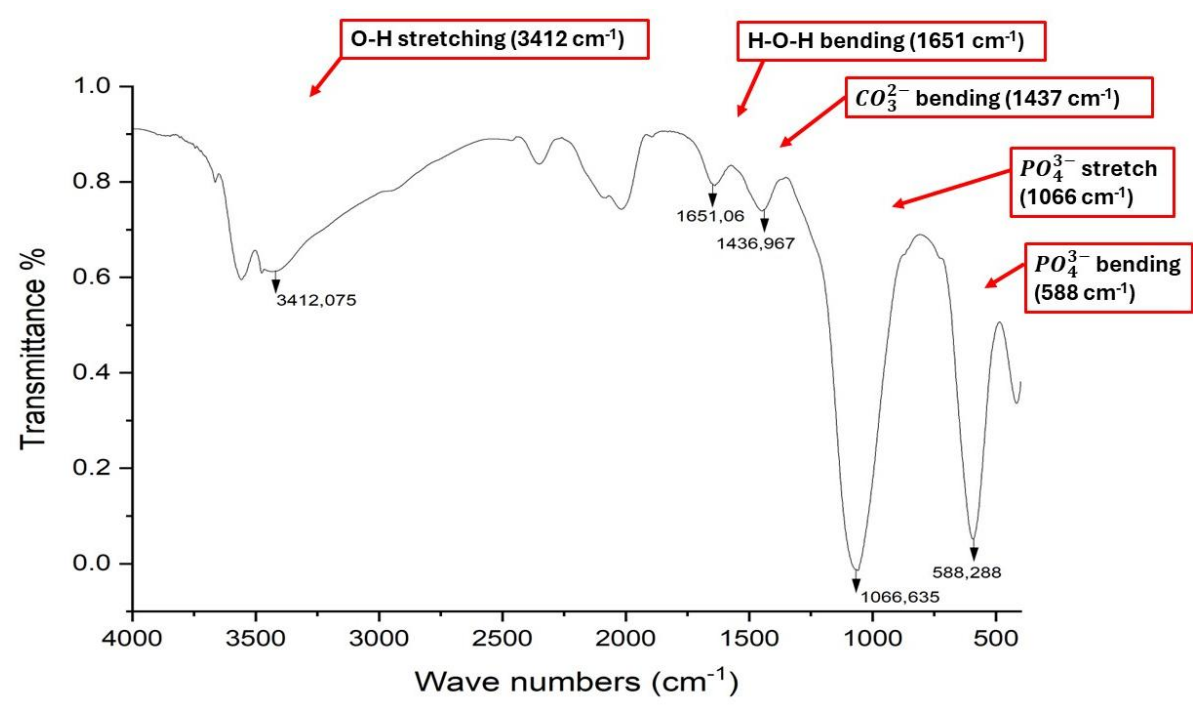


Figure 2. HAp Wave Number of Bukit Jimbaran Limestone

Figure 2 shows the FTIR spectrum of HAp synthesized from Bukit Jimbaran limestone. Strong absorption bands at 1066 cm⁻¹ and 588 cm⁻¹ are seen, which are associated with the stretching and bending vibration modes of the phosphate group (PO₄³⁻), respectively, indicating the formation of a typical hydroxyapatite structure. A broad absorption at 3412 cm⁻¹ indicates hydroxyl group stretching (O-H stretching), while the band at 1651 cm⁻¹ indicates H-O-H bending originating from a small amount of bound water or the presence of minor CaO. In addition, the band at 1437 cm⁻¹ indicates the presence of a carbonate group (CO₃²⁻). The presence of this band is a strong indication that carbonate substitution has occurred in the HAp lattice. Based on its position and intensity, the band around 1437 cm⁻¹ indicates a type B carbonate, which is the substitution of CO₃²⁻ ions to replace phosphate groups (PO₄³⁻). However, the appearance of a weak absorption around 3412 cm⁻¹ associated with O-H stretching and a slight shift in the position of the carbonate band indicates the presence of a type A carbonate component, where CO₃²⁻ ions replace hydroxyl groups (OH⁻). Thus, these FTIR results confirm the formation of a mixed type A and type B carbonate apatite (A-B-type carbonate apatite). The presence of both types of carbonate is often found in HAp synthesized from calcium carbonate precursors due to the carbonate-rich reaction conditions [26][27][28][29]. This carbonate-substitution structure is biomimetic, resembling natural bone mineral, and enhances the bioactivity and osteoconductivity of the material. To ensure that the carbonate bands were not the result of CO₂ adsorption from the air, the Ca/P ratio analysis from the EDX results was used as a reference. The Ca/P value approaching the stoichiometry of 1.67 confirmed that the detected carbonate was part of the apatite crystal structure, not surface contamination [30][31]. Therefore, the FTIR results supported by EDX data confirmed that the Bukit Jimbaran limestone HAp was formed as a mixed type carbonate apatite (A-B type carbonate apatite) with a dominance of type B [32].

Table 2. Comparison of Wavenur	nbers of HAp from Buki	t Jimbaran Lime	stone and HAp
from Limestone			

Identification of Chemical Functional Groups in	Hydroxyapatite from Bukit Jimbaran Limestone	HAp Derived from Limestone [27]		
HAp	Wavenumber (cm ⁻¹)			
Phosphate (PO_4^{3-})	588.288; 1066.635	580.32; 1131.96		
Calcium Oxide (CaO)	1651.06	1657.106		
Carbonate (CO_3^{2-})	1436.967	1400.08		
Hydroxyl (OH-)	3412.057	3412.48		

XRD analysis to confirm the crystal structure, crystal size, and degree of crystallinity. The next X-ray diffraction pattern is presented in Figure 3.

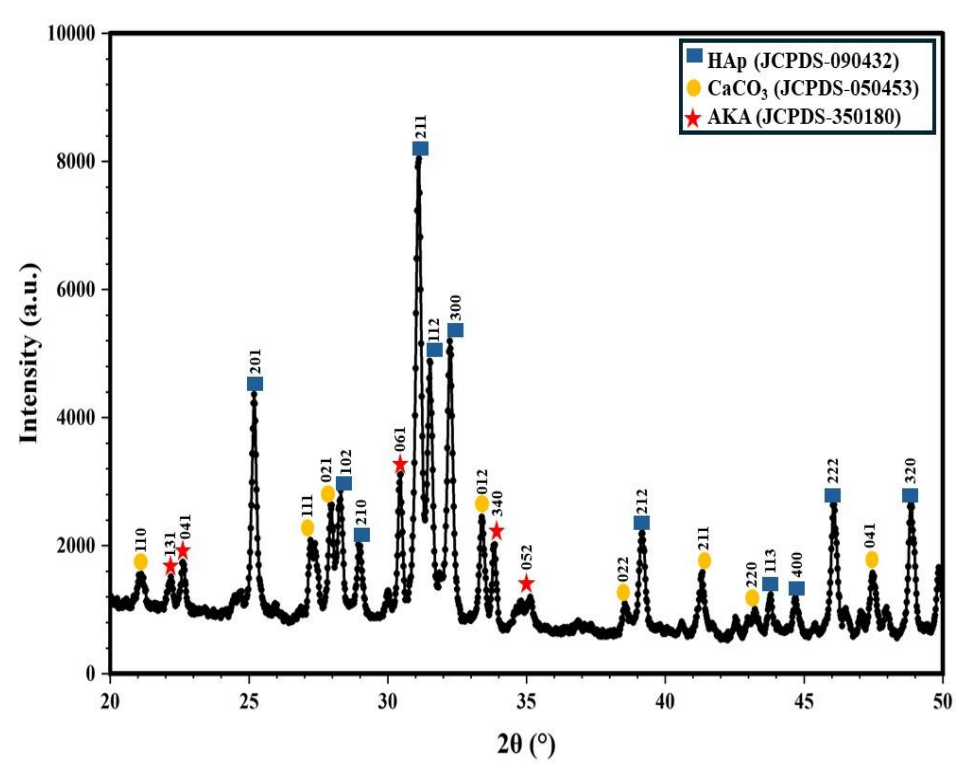


Figure 3. HAp Diffractogram of Jimbaran Limestone

The XRD pattern (Figure 3) shows the presence of several main crystalline phases, namely hydroxyapatite (HAp), calcium carbonate (CaCO₃), and type A carbonate apatite (AKA). The characteristic peaks of HAp were observed at angles $2\theta = 25.283^{\circ}$, 28.111° , 28.948° , 31.668° , 32.172° , 32.800° , 39.183° , 43.787° , 44.291° , 46.660° , and 48.863° , which correspond to the (hkl) planes (201), (102), (210), (211), (112), (300), (212), (113), (400), (222), and (320) based on JCPDS reference data No. 09-0432 for the compound $Ca_{10}(PO_4)_6(OH)_2$. In addition to the main HAp phase, additional peaks were also detected at $2\theta = 21.118^{\circ}$, 26.263° , 27.341° , 33.188° , 38.546° , 41.341° , 42.232° , 48.486° which correspond to the hkl planes (110), (111), (021), (012), (022), (211), (220), (041) identified as the CaCO₃ phase (JCPDS No. 05-0453) as well as the type A carbonate apatite (AKA) peak (JCPDS No. 35-0180) with $2\theta = 21.587^{\circ}$, 22.618° , 30.469° , 33.819° , 35.075° and hkl planes (131), (041), (061), (340), (052). The presence of CaCO₃ may originate

from the residual calcium carbonate that is not fully reacted or from the recarbonation of CaO during the synthesis process [33]. The presence of the carbonate peak indicates that carbonate ions (CO₃²⁻) have participated in the formation of the crystal structure, replacing some of the phosphate (PO₄³⁻) and hydroxyl (OH⁻) groups in the HAp lattice. The mixed type carbonate apatite phase (A–B-type carbonate apatite) is formed due to carbonate substitution at both the phosphate position (B-type) and the hydroxyl position (A-type). This finding is in line with the FTIR results (Figure 2), which show a characteristic CO₃²⁻ absorption band at 1437 cm⁻¹ and an O–H stretch at 3412 cm⁻¹ confirming the presence of double carbonate substitution. The presence of this mixed apatite structure shows biomimetic properties that resemble natural bone minerals, thus potentially increasing the bioactivity of the material [34][35][36][37]. From

Scherrer's calculations, the average crystal size was 8.70 nm. Meanwhile, the percentage of crystallinity calculated by the Landi method reached 92.88%. High crystallinity indicates that the HAp phase is perfectly formed due to the purity of the precursor, while the very small crystal size increases the surface area, which has an impact on increasing bioactivity and osteointegration [38]. The lattice parameters of Bukit Jimbaran limestone HAp are a = b = 9.45 Å and c = 6.85 Å, which indicate a hexagonal crystal structure. This value is in line with research [39], that the HAp crystal size is 97.7 nm with lattice parameters a = b = 9.4232 Å and c = 6.8833 Å confirming a hexagonal crystal structure. More details, a comparison of lattice parameters is shown in table 3.

Table 3. Comparison of HAp Lattice Parameters of Jimbaran Limestone with JCPDS-090432

Sample Name	Lattice a=b (Å)	Parameters c (Å)	Crystal Structure
Jimbaran Limestone HAp	9.45	6.85	Hexagonal
JCPDS 09-0432 Reference	9.418	6.884	Hexagonal

Morphological analysis and elemental composition using SEM-EDX at 1500× magnification shows the surface morphology of Bukit Jimbaran limestone HAp particles that are clumped or agglomerated. This finding is in line with research [40], which states that hydroxyapatite crystals form agglomerates caused by the rate of precipitation that causes particles to collide before they are surface stable and the effects of the oven and sintering processes. For mitigation in further studies, an approach was carried out through spray-drying and controlling the rate of reagent addition to reduce supersaturation during precipitation [35].

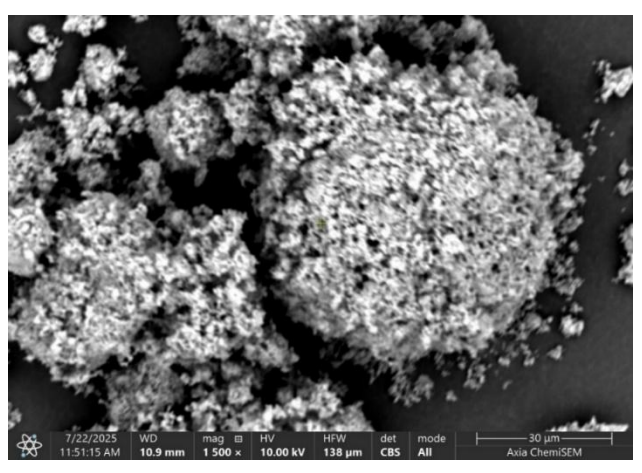


Figure 4. SEM Micrograph of Hap Limestone from Bukit Jimbaran

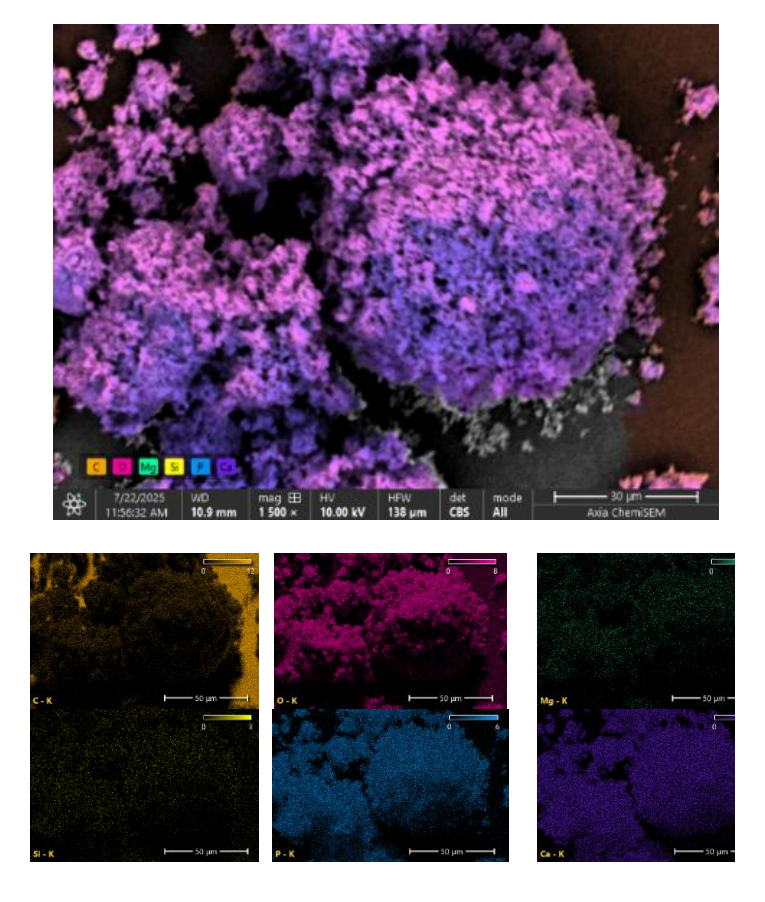


Figure 5. Distribution of HAp Elements in Jimbaran Limestone

EDX analysis (Figure 5) revealed a homogeneous elemental distribution dominated by Ca, P, O as shown in Table 4. The Ca/P ratio based on atomic percent (At.%) was 1.76, which is close to the ideal stoichiometric value of 1.67. The ratio of synthetic HAp was slightly higher due to the presence of minor $CaCO_3$ or residual CaO phases [41,42]. In addition, magnesium (Mg) and silicon (Si) elements were identified in small scale (<0.5%), where their presence is considered as natural doping that supports bioactivity without disturbing the main structure of HAp [28,29]

Table 4. Elements of Nanohydroxyapatite from Jimbaran-Bali Limestone

Element	Line	At. %	Wt. %	Net Counts	At. % Error	Wt. % Error
C	K	13.4	7.7	38 457	0.1	0.1
O	K	59.9	45.6	132 420	0.3	0.2
Mg	K	0.4	0.5	3 202	0.0	0.0
Si	K	0.1	0.2	1 108	0.0	0.0
P	K	9.5	14.0	77 487	0.1	0.1
Ca	K	16.7	32.0	71 879	0.1	0.2

Conclusion

Nanohydroxyapatite (Ca10(PO4)6(OH)2) was successfully synthesized by precipitation method using Bukit Jimbaran limestone with very high CaO purity (CaO = 99.62% based on XRF). FTIR analysis confirmed the functional groups of HAp, including B-type carbonate (CO₃2⁻), which is biomedically relevant because it mimics the structure of natural bone mineral, XRD results showed a hexagonal crystal structure with lattice parameters a = b = 9.45 Å and c = 6.85Å, and an average crystallite size of 8.70 nm with a crystallinity of 92.88%. SEM-EDX analysis showed that the particles tended to agglomerate, but the distribution of Ca, P, and O elements was homogeneous and in accordance with the stoichiometry of HAp. More broadly, this study confirms the potential of Bukit Jimbaran limestone, Bali, as a high-quality local resource for producing competitive, economically viable HAp for biomedical applications, particularly bone implants. These results have an impact on the development of locally sourced biomaterials to support the independence of the healthcare industry in Indonesia. However, this study still has limitations in the form of particle agglomeration, the absence of quantitative particle size distribution (PSA) analysis, and the absence of further biological testing. Therefore, future research needs to focus on synthesis optimization strategies (including controlling the precipitation rate, adjusting the stirring speed, and applying spray drying) to reduce agglomeration, as well as conducting in vitro/in vivo testing to evaluate the bioactivity and biocompatibility of the material.

Acknowledgment

This research was fully supported by the research supervisor and the facilities provided by the Advanced Physics Laboratory, Physical Chemistry Laboratory, and Research Laboratory of the Ganesha University of Education, as well as the Mineral and Advanced Materials Laboratory of the State University of Malang.

References

- [1] X. Mo, D. Zhang, K. Liu, X. Zhao, X. Li, and W. Wang, "Nano-Hydroxyapatite Composite Scaffolds Loaded with Bioactive Factors and Drugs for Bone Tissue Engineering," *Int. J. Mol. Sci.*, vol. 24, no. 2, pp. 1-30, 2023.
- [2] S. Aziz, I. D. Ana, Y. Yusuf, and H. D. Pranowo, "Synthesis of Biocompatible Silver-Doped Carbonate Hydroxyapatite Nanoparticles Using Microwave-Assisted Precipitation and In Vitro Studies for the Prevention of Peri-Implantitis," *J. Funct. Biomater.*, vol. 14, no. 7, pp. 1-14, 2023.
- [3] A. Keremu, M. Abulikemu, Z. Liang, A. Abulikemu, and A. Tuxun, "Anti-Infection Efficacy, Osteogenesis Potential, and Biocompatibility of 3D Printed PLGA/Nano-Hydroxyapatite Porous Scaffolds Grafted with Vancomycin/DOPA/rhBMP-2 in Infected Rabbit Bone Defects," *Int. J. Nanomedicine*, vol. 20, no. 1, pp. 6399-6421, 2025.
- [4] K. Sinulingga, M. Sirait, N. Siregar, and H. Abdullah, "Synthesis and Characterizations of Natural Limestone-Derived Nano-Hydroxyapatite (HAp): A Comparison Study of Different Metals Doped HAps on Antibacterial Activity," *RSC Adv.*, vol. 11, no. 26, pp. 15896–15904, 2021.
- [5] M. A. E. H. Adam, S. E. El-Shafey, and S. R. Mohamed, "Enhancing the Performance of SILRES® BS OH 100 as A Consolidant of Archaeological Limestone Using Nano-Hydroxyapatite," Egypt. J. Chem., vol. 66, no. 10, pp. 403–414, 2023.
- [6] X. Hou, L. Zhang, Z. Zhou, X. Luo, T. Wang, X. Zhao, B. Lu, F. Chen, and L. Zheng,

- "Calcium Phosphate-Based Biomaterials for Bone Repair," *J. Funct. Biomater.*, vol. 13, no. 4, pp. 1-39, 2022.
- [7] J. G. Lyons, M. A. Plantz, W. K. Hsu, E. L. Hsu, and S. Minardi, "Nanostructured Biomaterials for Bone Regeneration," *Front. Bioeng. Biotechnol.*, vol. 8, no. 1, pp. 1–28, 2020.
- [8] A. M. de Souza, H. Araujo-Silva, A. M. Costa, A. L. Rossi, A. M. Rossi, J. M. Granjeiro, A. C. Luchiari, and S. R. B. de Medeiros, "Embryotoxicity and Visual-Motor Response of Functionalized Nanostructured Hydroxyapatite-Based Biomaterials in Zebrafish (Danio rerio)," *Chemosphere*, vol. 313, no. 1, pp. 1-11, 2022.
- [9] R. P. Alanis-Gomez, F. Mernandez-Rosas, J. D. Olivares-Hernandez, E. M. Rivera-Munoz, A. Zapatero-Gutierrez, N. Mendez-Lozano, J. R. Alanis-Gomez, and R. Velazquez-Castillo, "Magnesium-Doped Hydroxyapatite Nanofibers for Medicine Applications: Characterization, Antimicrobial Activity, and Cytotoxicity Study," *Int. J. Mol. Sci.*, vol. 25, no. 22, pp. 1-26, 2024.
- [10] K. Jarquin-Yanez, E. Rubio-Rosas, G. Pinon-Zarate, A. Castell-Rodriguez, and M. Poisot, "Cellulose-Chitosan-Nanohydroxyapatite Hybrid Composites by One-Pot Synthesis for Biomedical Applications," *polymers*, vol. 13, no. 1, pp. 1–13, 2021.
- [11] G. Ulian, D. Moro, and G. Valdrè, "Hydroxylapatite and Related Minerals in Bone and Dental Tissues: Structural, Spectroscopic and Mechanical Properties from a Computational Perspective," *Biomolecules*, vol. 11, no. 5, pp. 1-34, 2021.
- [12] A. Anil, W. I. Ibraheem, A. A. Meshni, R. S. Preethanath, and S. Anil, "Nano-Hydroxyapatite (nHAp) in the Remineralization of Early Dental Caries: A Scoping Review," *Int. J. Environ. Res. Public Health*, vol. 19, no. 9, pp. 1-14, 2022.
- [13] Y. Wu, S. Chen, P.Luo, S. Deng, Z. Shan, J. Fang, X. Liu, J. Xie, R. Liu, S. Wu, X. Wu, Z. Chen, K. W. K. Yeung, Q. Liu, and Z. Chen, "Optimizing the Bio-Degradability and Biocompatibility of a Biogenic Collagen Membrane through Cross-Linking and Zinc-Doped Hydroxyapatite," *Acta Biomater.*, vol. 143, no. 1, pp. 159–172, 2022.
- [14] R. S. M. Chan, S. J. Lee, F. W. T. Zhou, R. Kishan, H. C. Shum, W. Yang, Y. Su, J. K. H. Tsoi, A. D. Diwan, B. G. Prusty, and K. Cho, "Engineered 3D-Printable Nanohydroxyapatite Biocomposites with Cold Plasma-Tailored Surface Features to Boost Osseointegration," ACS Appl. Mater. Interfaces, vol. 17, no. 16, pp. 23522–23535, 2025.
- [15] I. A. Suci and Y. D. Ngapa, "Sintesis dan Karakterisasi Hidroksiapatit dari Cangkang Kerang Ale-Ale Menggunakan Metode Presipitasi Double Stirring," *Cakra Kim.*, vol. 8, no. 2, pp. 73–81, 2020.
- [16] F. Afifah and S. E. Cahyaningrum, "Synthesis and Characterization of Hydroxyapatite from Cow Bones (*Bos Taurus*) Using Calcination Techniques," *UNESA J. Chem.*, vol. 9, no. 3, pp. 189–196, 2020.
- [17] K. Sinulingga and M. Sirait, "Hasil Penelitian dan Pembahasan," in *Hidroksiapatit dari Batu Kapur dan Aplikasi*, Medan, Indonesia: Yayasan Kita Menulis, 2021, ch.4, pp. 31-41.
- [18] M. K. Alam, M. S. Hossain, M. K. N. M. Bahadur, and S. Ahmed, "Synthesis of Nano-Hydroxyapatite Using Emulsion, Pyrolysis, Combustion, and Sonochemical Methods and Biogenic Sources: A Review," *RSC Adv.*, vol. 14, no. 5, pp. 3548–3559, 2024.
- [19] Y. Inayah, A. S. P. Anggraeni, and A. D. Karisma, "Pembuatan Biokompatibel Komposit

- dari Nano Hidroksiapatit Berbahan Dasar Cangkang Keong Sawah (*Pila ampullacea*) dengan Kombinasi Biopolimer PVA (*Polyvinyl Alcohol*) sebagai Bahan Dasar Pembuatan Suture Anchor," *J. Teknol.*, vol. 11, no. 1, pp. 58–66, 2023.
- [20] N. S. Andyana, A. R. Amalia, and K. Sumada, "Kajian Hidroxyapatite dari Cangkang Kupang Putih dan Asam Fosfat," *Chempro*, vol. 2, no. 3, pp. 1–6, 2021.
- [21] S. K. Padmanabhan, P. Nitti, E. Stanca, A. Rochira, L. Siculella, M. Grazia Raucci, M. Madaghiele, A. Licciulli, and C. Demitri, "Mechanical and Biological Properties of Magnesium and Silicon Substituted Hydroxyapatite Scaffolds," *Materials.*, vol. 14, no. 22, pp. 1-16, Nov. 2021.
- [22] W. J. M. Bay and L. Pulungan, "Pemanfaatan Bahan Galian Mineral Kalsit Berdasarkan Karakteristik Sifat Fisik di Cikembar Sukabumi," *J. Ris. Tek. Pertamb.*, vol. 2, no. 1, pp. 41–48, 2022.
- [23] C. A. Asnur, M. I. Juradi, and M. Arifin, "Analisis Komposisi Kimia Batugamping di Daerah Leang-Leang Kabupaten Maros," *J. Energy Miner. Resour.*, vol. I, no. 1, pp. 1–8, 2023.
- [24] F. M. Gasperini, G. V. O. Fernandes, F. F. M. M. D. Calasans-Maia, E. Mavropoulos, A. M. Rossi, and J. M. Granjeiro, "Histomorphometric Evaluation, SEM, and Synchrotron Analysis of the Biological Response of Biodegradable and Ceramic Hydroxyapatite-Based Grafts: From the Synthesis to the Bed Application," *Biomed. Mater.*, vol. 18, no. 6, pp. 1-16, 2023.
- [25] N. H. Alotaibi, M. U. Munair, N. K. Alruwaili, K. S. Alharbi, A. I. A. S. Almurshedi, I. U. Khan, S. N. A. Bukhari, and M. Rehman, "Synthesis and Characterization of Antibiotic–Loaded Biodegradable Citrate Functionalized Mesoporous Hydroxyapatite Nanocarriers as an Alternative Treatment for Bone Infections," *Pharmaceutics*, vol. 14, no. 5, pp. 1-13, 2022.
- [26] M. Sirait and M. Aulia, "Sintesis dan Uji Sitotoksisitas Hidroksiapatit Batu Kapur Sebagai Bahan Graft Tulang," *J. Einstein*, vol. 9, no. 3, pp. 18-25, 2021.
- [27] T. ATEŞ, S. KESER, A. A. KORKMAZ, N. BULUT, and O. KAYGİLİ, "NiO Takviyeli Mn Katkılı Hidroksiapatit Kompozitlerinin Sentez ve Karakterizasyonu," *Int. J. Innov. Eng. Appl.*, vol. 6, no. 1, pp. 48–54, 2022.
- [28] F. E. BAŞTAN, O. KARAARSLAN, and F. ÜSTEL, "Biyomedikal Uygulamalar için Wollastonit Partikül Takviyeli Hidroksiapatit Kompozit Granüllerin Üretilmesi ve Karakterizasyonu," *Deu Muhendis. Fak. Fen ve Muhendis.*, vol. 23, no. 67, pp. 1–9, 2021.
- [29] A.L. Rosa, L. R. Farias, V. P. Dias, O. B. Pacheco, F. D. P. Morisso, L. F. Rodrigues, M. R. Sagrillo, A. Rossato, L. L. Santos, and T. M. Volkmer, "Effect of Synthesis Temperature on Crystallinity, Morphology and Cell Vibability of Nanostructured Hydroxyapatite Via Wet Chemical Precipitation Method," *Int. J. Adv. Med. Biotechnol.*, vol. 5, no. 1, pp. 29-35, 2022.
- [30] M. Sirait, K. Sinulingga, N. Siregar, and Y. F. Damanik, Synthesis and Characterization of Hydroxyapatite From Broiler Eggshell: Open The 1st International Conference on Physics and Applied Physics (The 1st ICP&AP), March 31 2020, Medan, Indonesia.
- [31] R. Bemis, Heriyanti, Rahmi, R. D. Puspitasari, and D. Imawati, "Pengaruh Variasi Konsentrasi Alumina Pada Sintesis Nanokomposit Hidroksiapatit/ Alumina dari Udang Papai Menggunakan Metode Hidrotermal," J. Indones. Soc. Integr. Chem., vol. 15,

- no. 1, pp. 56-66, 2023.
- [32] K. Niziołek, D. Słota, J. Sadlik, E. Łachut, W. Florkiewicz, and A. Sobczak-Kupiec, "Influence of Drying Technique on Physicochemical Properties of Synthetic Hydroxyapatite and Its Potential Use as a Drug Carrier," *Materials (Basel).*, vol. 16, no. 19, pp. 1-12, 2023.
- [33] S. Belouafa, H. Chaair, and K. Digua, "Oxygenated Apatites: Effect of Calcium Salt Nature and Synthesis Parameters," vol. 14, no. 4, pp. 26–33, 2022.
- [34] K. Benataya, M. Lakrat, O. Hammani, M. Aaddouz, Y. Ait Yassine, H. A. Abuelizz, A. Zarrouk, K. Karrouchi, and E. Mejdoubi, "Synthesis of High-Purity Hydroxyapatite and Phosphoric Acid Derived from Moroccan Natural Phosphate Rocks by Minimizing Cation Content Using Dissolution-Precipitation Technique," *Molecules*, vol. 29, no. 16, pp. 1-15, 2024.
- [35] M. Eriksson, K. Sandström, M. Carlborg, and M. Broström, "Impact of Limestone Surface Impurities on Quicklime Product Quality," *Minerals*, vol. 14, no. 3, pp. 1–13, 2024.
- [36] V. S. Bystrov, E. V. Paramonova, L. A. Avakyan, N. V. Eremina, S. V. Makarova, and N. V. Bulina, "Effect of Magnesium Substitution on Structural Features and Properties of Hydroxyapatite," *Materials.*, vol. 16, no. 17, pp. 1-26, 2023.
- [37] M. Safarzadeh, S. Ramesh, and C. Y. Tan, "Sintering behaviour of carbonated hydroxyapatite prepared at different carbonate and phosphate ratios," *Bol. la Soc. Esp. Ceram. y Vidr.*, vol. 38, no. 7, pp. 1807–1819, 2020.
- [38] H. Copete, E. López, and C. Baudin, "Synthesis and Characterization of B-Type Carbonated Hydroxyapatite Materials: Effect of Carbonate Content on Mechanical Strength and In vitro Degradation," *Bol. la Soc. Esp. Ceram. y Vidr.*, vol. 63, no. 4, pp. 255–267, 2023.
- [39] K. Benataya, M. Lakrat, L. L. Elansari, and E. Mejdoubi, "Synthesis of B-type carbonated hydroxyapatite by a new dissolution-precipitation method," *Mater. Today Proc.*, vol. 31, no. 2, pp. S83–S88, 2020.
- [40] H. A. Permatasari, M. Sari, Aminatun, T. Suciati, K. Dahlan, and Y. Yusuf, "Nanocarbonated hydroxyapatite precipitation from abalone shell (Haliotis asinina) waste as the bioceramics candidate for bone tissue engineering," *Nanomater. Nanotechnol.*, vol. 11, pp. 1–9, 2021.